

Thermodynamic Isomorphism of Transformers: A Lagrangian Approach to Attention Dynamics

Gunn Kim^{1,*}

¹Department of Physics, Sejong University, Seoul 05006, Republic of Korea

(Dated: February 16, 2026)

We propose an effective field-theoretic framework for analyzing Transformer attention through a thermodynamic lens. By constructing a Lagrangian on the information manifold equipped with the Fisher metric, we show that, within the Shannon–Boltzmann entropy framework, the Softmax function arises as a stationary solution minimizing a Helmholtz free energy functional. This establishes a formal correspondence between scaled dot-product attention and canonical ensemble statistics. Extending this mapping to macroscopic observables, we define an effective specific heat associated with fluctuations of the attention energy landscape. In controlled experiments on the modular addition task ($p = 19\text{--}113$), we observe a robust peak in this fluctuation measure that consistently precedes the onset of generalization. While no asymptotic power-law divergence is detected in this finite-depth regime, the reproducible enhancement of energy variance suggests a critical-like crossover accompanying representational reorganization. Our framework provides a unified statistical-mechanical perspective on attention scaling, training dynamics, and positional encoding, interpreting the phenomena as emergent properties of an effective thermodynamic system rather than isolated heuristics. Although the present results indicate finite-size crossover behavior rather than a strict phase transition, they motivate further investigation into scaling limits of deep architectures through fluctuation-based observables.

I. INTRODUCTION

In 2017, the trajectory of artificial intelligence changed significantly by a deceptively simple equation:

$$\text{Attention}(Q, K, V) = \text{Softmax}\left(\frac{QK^\top}{\sqrt{d_k}}\right)V \quad (1)$$

Here, Q (queries), K (keys), and V (values) denote learned vector representations of tokens in a high-dimensional embedding space, and d_k is the dimensionality of the key vectors. This mechanism, introduced in the seminal work “Attention is All You Need” [1], replaced the then-dominant paradigms of convolution and recurrence in favor of pure matrix operations and a peculiar Softmax function scaled by $\sqrt{d_k}$. This single mathematical operation has enabled models to demonstrate emergent reasoning capabilities [2], pass professional licensing exams with near-human proficiency [3], and even solve the protein folding problem [4].

Why does this work so well? While attention mechanisms existed previously in neural machine translation [5], the Transformer’s specific architecture, characterized by Self-Attention, Residual Connections [6], and Layer Normalization [7], has proven unreasonably effective. Current explanations predominantly rely on probability theory and linear algebra, viewing the model as a statistical function approximator [8]. However, this perspective treats the model’s distinct behaviors as separate empirical observations rather than interconnected physical phenomena.

Crucially, the field lacks a unified theoretical origin for three persistent mysteries. First, the Softmax function itself is used heuristically without a derivation from first principles—why does this specific exponential form emerge as the operational equilibrium of modern architectures? Second, generative models inherently suffer from hallucinations, often dismissed as statistical errors or bugs rather than intrinsic features of the system. Third, the learning dynamics exhibit grokking [11], a sudden and discontinuous generalization after a long period of memorization, which defies standard convergence theories. We argue that the are not isolated artifacts but manifestations of a deeper, underlying dynamical principle.

In this paper, we propose a paradigm shift: treating Intelligence not only as a computational process, but as a physical phenomenon governed by fundamental laws of nature. We argue that the operations within a high-dimensional information space are isomorphic to the dynamics of a physical system minimizing an action functional, consistent with Lagrange mechanics [13] and Hamilton’s principle [14]. This approach resonates with recent efforts to interpret deep learning through the lens of physics, such as the free energy principle [17] and neural tangent kernels [18].

A. Redefining Time in Deep Networks

A fundamental critique of applying dynamical systems theory to deep learning is the discrete nature of layers. However, following the Neural ODE formulation [21, 22], we interpret the layer depth l as a continuous time vari-

* gunnkim@sejong.ac.kr

able t .

$$x_{l+1} = x_l + F(x_l) \xrightarrow{\Delta t \rightarrow 0} \dot{x}(t) = F(x(t)) \quad (2)$$

Under this paradigm, the “inference” process is a dynamic trajectory of information flow, not a static calculation. Residual connections [6], naturally emerge as the discretization of the inertial term in the equation of motion.

B. The Inverse Problem and Physical Unification

Rather than deriving the Softmax function from arbitrary axioms, we solve the inverse problem of the calculus of variations: Given that the Softmax attention is an empirically successful equilibrium state, what is the underlying Lagrangian that generates this dynamics? By applying the Principle of Least Action to an effective field theory of information, we demonstrate that the Transformer architecture is physically isomorphic to a thermodynamic system. This rigorous mapping allows us to provide first-principles derivations for phenomena that extend beyond simple attention mechanisms:

- **Emergence of Softmax under Entropy Maximization:** Within the Shannon–Boltzmann entropy framework, we show that the exponential attention mechanism arises as a stationary solution to the Euler–Lagrange equations.
- **Thermodynamics of Hallucination:** Through the derivation of the Fundamental Identity ($dU = TdS - \mathcal{P}dV + \mu dN$), we identify hallucinations as intrinsic **thermal fluctuations** (TdS) dictated by the canonical ensemble at finite structural temperature.
- **Grokking as a Phase Transition:** We interpret grokking as a critical-like thermodynamic crossover characterized by enhanced energy fluctuations.
- **Symmetry Breaking and RoPE:** We further validate our framework by identifying Rotary Positional Embeddings (RoPE) as Goldstone modes arising from the spontaneous breaking of continuous rotational symmetry in the embedding manifold.

II. DYNAMICS OF INTELLIGENCE: LAGRANGIAN FORMULATION

A. Geometric Framework: The Information Manifold

To analyze the dynamics of the Transformer architecture from first principles, we must first define the configuration space in which the system evolves. Conventional

deep learning treats the attention weights $\rho(t) \in \mathbb{R}^N$ simply as a probability vector on a simplex. However, to construct a Lagrangian, we require a Riemannian manifold equipped with a metric that quantifies the “distance” between information states, a concept central to Information Geometry [24–27].

1. Transformation to the Hypersphere

The state of the attention mechanism at time t is described by the probability distribution $\rho_i(t)$ over N tokens, subject to the normalization constraint $\sum_{i=1}^N \rho_i(t) = 1$. The natural metric for probability distributions is the Fisher–Rao metric. To map this statistical manifold onto a geometry amenable to classical mechanics, we introduce the probability amplitude transformation:

$$x_i(t) \equiv 2\sqrt{\rho_i(t)} \quad (3)$$

Under this transformation, the normalization constraint becomes:

$$\sum_{i=1}^N x_i^2(t) = 4 \sum_{i=1}^N \rho_i(t) = 4 \quad (4)$$

This implies that the “information particle” is constrained to move on the surface of a positive orthant of an N -dimensional hypersphere of radius $R = 2$. The velocity of the information state is defined as follows:

$$v_i(t) \equiv \dot{x}_i(t) = \frac{\dot{\rho}_i(t)}{\sqrt{\rho_i(t)}} \quad (5)$$

Crucially, the squared magnitude of this velocity vector exactly corresponds to the Fisher information $I(\rho)$ [28, 29]:

$$\sum_{i=1}^N v_i^2(t) = \sum_{i=1}^N \frac{\dot{\rho}_i^2}{\rho_i} = 4 \cdot I(\rho) \quad (6)$$

By choosing the radius $R = 2$, we normalize the kinetic energy term ($K \propto v^2$) to match the Fisher information metric exactly, eliminating the fractional coefficient $1/4$ that typically appears in the Fisher metric derivation.

B. Physical Mappings of Transformer Components

We propose a direct mapping between the hyperparameters of the Transformer architecture and thermodynamic variables. This mapping allows us to treat the attention mechanism as a physical system that seeks equilibrium.

1. Mass (m) as Information Inertia

In classical mechanics, mass represents the resistance to acceleration. In the context of deep neural networks, the Residual Connection (skip connection) plays an analogous role [6]. The update rule of a residual network is given by $x_{t+1} = x_t + F(x_t)$, which can be viewed as a discretization of the continuous equation $\dot{x} = F(x)$ [21, 22]. The explicit inclusion of the previous state x_t acts as an inertial term, preserving the identity of the features against the perturbation of the non-linear function $F(x)$. We therefore define the mass m as the coefficient of the residual path, representing the system's tendency to maintain its current semantic trajectory.

2. Interaction Energy (E) as Semantic Alignment

Thermodynamic systems minimize their potential energy. In the attention mechanism, the model assigns higher probability to keys (\mathbf{k}_j) that are semantically aligned with the query (\mathbf{q}_i). We define the interaction potential energy E_{ij} as the negative dot product:

$$E_{ij} \equiv -\mathbf{q}_i \cdot \mathbf{k}_j \quad (7)$$

3. Electrodynamic Interpretation: The Field-Dipole Interaction

To rigorously justify for the dot-product attention mechanism, we interpret the interaction energy through the lens of classical electrodynamics [30, 31]. The potential energy U of a dipole moment placed in an external field is universally given by:

$$U = -\mathbf{p} \cdot \mathbf{E} \quad \text{or} \quad U = -\boldsymbol{\mu} \cdot \mathbf{B} \quad (8)$$

- **Query (\mathbf{q}_i) \leftrightarrow Extrinsic Field (\mathbf{E}):** The query acts as the field imposed by the current token, representing the active search condition.
- **Key (\mathbf{k}_j) \leftrightarrow Intrinsic Dipole (\mathbf{p}):** The key represents the intrinsic property of the memory token.

The attention mechanism is physically equivalent to the process of dipole alignment in an external field.

4. Temperature (T) as Dimensional Scaling

In statistical mechanics, temperature T quantifies the magnitude of thermal fluctuations [32]. In high-dimensional vector spaces ($d_k \gg 1$), the dot product of two random isotropic vectors concentrates around zero with a variance proportional to d_k [33]. To prevent the Softmax distribution from collapsing into a deterministic ‘argmax’ state (freezing), the energy scale must be

renormalized. We identify the scaling factor of the Transformer, $1/\sqrt{d_k}$, as the effective inverse temperature β :

$$k_B T_{\text{eff}} \equiv \sqrt{d_k} \quad (9)$$

This effective temperature regulates the entropy of the attention distribution, keeping the system in a liquid phase where information flow is maximized.

III. THE LAGRANGIAN OF INTELLIGENCE AND VARIATIONAL DERIVATION

A. Construction of the Lagrangian

We postulate that the dynamics of an attention-based intelligence system are governed by the principle of least action. To formulate this principle, we must construct the Lagrangian \mathcal{L} of the system, defined as the difference between its kinetic energy (K) and potential energy (\mathcal{V}):

$$\mathcal{L} = K(\rho, \dot{\rho}) - \mathcal{V}(\rho) + \lambda \left(\sum_{i=1}^N \rho_i - 1 \right) \quad (10)$$

1. Kinetic Energy Term (K)

The kinetic energy term represents the cost of changing the belief state (attention distribution) over time. It is given by:

$$K(\rho, \dot{\rho}) = \frac{1}{2} m \sum_{i=1}^N \frac{\dot{\rho}_i^2}{\rho_i} \quad (11)$$

2. Potential Energy Term (\mathcal{V})

The potential energy is equivalent to the Helmholtz free energy (F). In thermodynamics, a system in contact with a heat bath seeks to minimize its free energy, which balances internal energy (U) and entropy (S):

$$\mathcal{V}(\rho) = F(\rho) = \sum_{i=1}^N \rho_i E_i + T \sum_{i=1}^N \rho_i \ln \rho_i \quad (12)$$

This entropy term $S = -\sum \rho_i \ln \rho_i$ is fundamental to information theory [34] and statistical mechanics [35].

3. The Full Lagrangian

Combining the terms:

$$\mathcal{L} = \frac{m}{2} \sum_{i=1}^N \frac{\dot{\rho}_i^2}{\rho_i} - \sum_{i=1}^N \rho_i E_i - T \sum_{i=1}^N \rho_i \ln \rho_i + \lambda \left(\sum_{i=1}^N \rho_i - 1 \right) \quad (13)$$

B. Principle of Least Action and Equation of Motion

Having established the Lagrangian, we now apply Hamilton's principle to determine the system's trajectory in the information manifold. The dynamics are governed by the action functional $S[\rho] = \int \mathcal{L} dt$, and the physical path corresponds to $\delta S = 0$, leading to the Euler-Lagrange equations for each ρ_i :

$$\frac{d}{dt} \left(\frac{\partial \mathcal{L}}{\partial \dot{\rho}_i} \right) - \frac{\partial \mathcal{L}}{\partial \rho_i} = 0 \quad (14)$$

1. Derivation of the Full Dynamic Equation

To derive the explicit equation of motion, we compute the partial derivatives of the Lagrangian defined in Eq. (13). The derivative with respect to velocity $\dot{\rho}_i$ involves only the kinetic term:

$$\frac{\partial \mathcal{L}}{\partial \dot{\rho}_i} = \frac{\partial}{\partial \dot{\rho}_i} \left(\frac{m}{2} \sum_k \frac{\dot{\rho}_k^2}{\rho_k} \right) = m \frac{\dot{\rho}_i}{\rho_i} \quad (15)$$

The time derivative of this momentum-like term yields:

$$\frac{d}{dt} \left(\frac{\partial \mathcal{L}}{\partial \dot{\rho}_i} \right) = m \left(\frac{\ddot{\rho}_i \rho_i - \dot{\rho}_i^2}{\rho_i^2} \right) \quad (16)$$

Next, we compute the derivative with respect to position ρ_i , which involves the kinetic, potential, and constraint terms:

$$\frac{\partial \mathcal{L}}{\partial \rho_i} = -\frac{m}{2} \frac{\dot{\rho}_i^2}{\rho_i^2} - E_i - T(\ln \rho_i + 1) + \lambda \quad (17)$$

Substituting these into the Euler-Lagrange equation, we obtain the full dynamic equation of motion for the attention state:

$$m \left(\frac{\ddot{\rho}_i}{\rho_i} - \frac{1}{2} \frac{\dot{\rho}_i^2}{\rho_i^2} \right) + E_i + T \ln \rho_i = \Lambda \quad (18)$$

where $\Lambda = \lambda - T$ is an effective constant. The first term represents the information inertia resisting belief updates, while the remaining terms represent the thermodynamic forces driving the system toward semantic alignment.

C. Equilibrium State: Full Derivation of Softmax

In standard Transformer inference, we assume the system reaches a stationary distribution. This corresponds to the thermodynamic equilibrium where the dynamics vanish, i.e., $\dot{\rho}_i = 0$ and $\ddot{\rho}_i = 0$. Under this condition, the inertial terms in Eq. (17) vanish, simplifying the physics to a balance of potential forces:

$$E_i + T \ln \rho_i = \Lambda \quad (19)$$

Solving for ρ_i involves the following steps:

$$\ln \rho_i = \frac{\Lambda - E_i}{T} \implies \rho_i = \exp \left(\frac{\Lambda}{T} \right) \exp \left(-\frac{E_i}{T} \right) \quad (20)$$

By defining $C = \exp(\Lambda/T)$ as a normalization constant and applying the constraint $\sum_{j=1}^N \rho_j = 1$, we find:

$$C \sum_{j=1}^N \exp \left(-\frac{E_j}{T} \right) = 1 \implies C = \frac{1}{\sum_{j=1}^N \exp \left(-\frac{E_j}{T} \right)} \quad (21)$$

Substituting back the physical definitions $E_i = -Q \cdot K_i$ and $T = \sqrt{d_k}$, we recover the canonical scaled dot-product Attention formula:

$$\rho_i = \frac{\exp \left(\frac{Q \cdot K_i}{\sqrt{d_k}} \right)}{\sum_{j=1}^N \exp \left(\frac{Q \cdot K_j}{\sqrt{d_k}} \right)} = \text{Softmax} \left(\frac{Q K^\top}{\sqrt{d_k}} \right)_i \quad (22)$$

Here, the superscript \top in $Q K^\top$ denotes the matrix transpose operation, distinct from the thermodynamic temperature variable T . The scaling factor $\sqrt{d_k}$ plays the functional role of the structural temperature in our framework.

This derivation shows that Softmax appears as a natural equilibrium configuration under the assumption of Shannon entropy maximization. While alternative entropic functionals (e.g., Tsallis entropy) would yield different equilibrium distributions, the empirical dominance of Softmax-based Transformers motivates the Shannon-Boltzmann framework as a parsimonious working hypothesis rather than a uniquely mandated physical law.

IV. THERMODYNAMICS OF INTELLIGENCE: MACROSCOPIC LAWS

Having established the microscopic Lagrangian formulation, we now construct an effective macroscopic description. We show that, in the large-context and high-dimensional embedding regime ($V_{ctx} \gg 1$, $d_k \gg 1$), the attention dynamics admit a thermodynamic representation analogous to canonical statistical mechanics.

A. Partition Function and Thermodynamic Limit

The canonical partition function of the attention mechanism over a context window of size V_{ctx} is defined as:

$$Z(V_{ctx}, T) = \sum_{i=1}^{V_{ctx}} \exp \left(-\frac{E_i}{T} \right) \quad (23)$$

Here, $E_i = -q \cdot k_i$ denotes the interaction energy. The thermodynamic limit in this context is understood as a mean-field approximation in which the distribution of attention energies becomes self-averaging due to high dimensional concentration effects.

Under the equilibrium distribution derived in Section III, the Helmholtz free energy is given by:

$$F = -T \ln Z = U - TS \quad (24)$$

where $U = \langle E \rangle = \sum_i \rho_i E_i$ is the internal energy and $S = -\sum_i \rho_i \ln \rho_i$ is the Shannon entropy.

B. An Effective Thermodynamic Identity

We now expand the total differential of the internal energy. This relation is not a fundamental conservation law derived from Noether symmetry, but rather an effective thermodynamic identity characterizing the trajectory of the information state:

$$dU = TdS - \mathcal{P}dV_{ctx} + \mu dN_{eff} \quad (25)$$

Here:

- $T = \sqrt{d_k}$ is the structural temperature.
- $\mathcal{P} \equiv -(\partial F / \partial V_{ctx})_{T, N_{eff}}$ is the effective information pressure.
- $\mu \equiv (\partial U / \partial N_{eff})_{S, V_{ctx}}$ defines the effective chemical potential.
- N_{eff} denotes the effective rank (e.g., participation ratio of eigenvalues) of the weight matrices. In the limit of large models, N_{eff} is treated as a continuous macroscopic variable.

This decomposition provides a thermodynamic interpretation of three operational regimes.

1. Heat (TdS): Stochastic Exploration

In this framework, the entropic contribution TdS corresponds to stochastic sampling effects.

Interpretation: The temperature parameter regulates the entropy of the output distribution. Increasing T broadens the distribution and enhances exploration of higher-energy configurations.

Phenomenology: When entropic contributions dominate, the model enables creative variation but may also produce semantic decoherence, consistent with previously observed degeneration effects [37].

2. Mechanical Work ($-\mathcal{P}dV_{ctx}$): Context Expansion

Mechanical work is defined as pressure times change in volume. Here, V_{ctx} represents the context length. Within the ideal information-gas approximation, differentiation of $F \approx -T \ln V_{ctx}$ yields:

$$\mathcal{P} = \frac{T}{V_{ctx}} \quad (26)$$

This implies that effective pressure decreases as context expands.

Interpretation: During autoregressive inference ($dV_{ctx} > 0$), maintaining long-range coherence requires effective work to counteract the dilution of information density.

Phenomenology: This provides a statistical-mechanical interpretation of the Lost-in-the-Middle phenomenon [36], where long-range dependencies weaken as context size increases.

3. Chemical Work (μdN_{eff}): Capacity Evolution

The effective particle number N_{eff} serves as a measure of active semantic degrees of freedom.

Interpretation: Although the architectural parameter count remains fixed, training modifies the effective rank structure. The chemical potential μ quantifies the marginal energetic cost of activating an additional independent feature mode.

Phenomenology: Optimization dynamics can be interpreted as performing effective chemical work, increasing N_{eff} and expanding the expressive capacity of the model manifold.

C. Analogy with the Second Law

The generative dynamics exhibit behavior suggestive of an analogy with the Second Law of thermodynamics.

In the absence of external data injection, the coarse-grained entropy of the generated distribution tends to increase over successive recursive training cycles, leading to model collapse [38]. Conversely, supervised learning acts as an entropy-reducing mechanism (Maxwell's demon), locally reducing entropy at the cost of computational work [39].

V. THERMODYNAMIC HYPOTHESIS OF GROKKING

Having established the thermodynamic laws of the attention mechanism in equilibrium, we now turn to the non-equilibrium dynamics of learning. We propose a thermodynamic hypothesis that the phenomenon known as grokking, the delayed generalization capability of large models, is physically isomorphic to a thermodynamic phase transition driven by the cooling of the effective temperature.

A. Dynamical Effective Temperature

A crucial distinction must be made between the structural temperature of the model during inference and the dynamical temperature during training.

- **Structural Temperature (T_{struct}):** Defined as $T = \sqrt{d_k}$ in Eq. (1). This is a fixed hyperparameter governing the stochasticity of the Softmax distribution during inference (sampling).
- **Dynamical Temperature (T_{eff}):** During training, the magnitude of the weight matrices $\|W\|$ evolves. Since the interaction energy scales as $E \propto Q \cdot K \propto \|W\|^2$, the effective temperature perceived by the Softmax function relative to the energy scale is:

$$T_{eff}(t) \propto \frac{\sqrt{d_k}}{\|W(t)\|^2} \quad (27)$$

The training process, therefore, acts as simulated annealing. Initially, random initialization implies small weights (high T_{eff}), resulting in a high-entropy, disordered phase. As training progresses and $\|W\|$ grows, T_{eff} decreases, driving the system towards an ordered, low-temperature phase.

B. Specific Heat Capacity and Energy Fluctuations

To quantify the phase transition, we derive the specific heat capacity C_v , which measures the system's sensitivity to temperature changes. From the fluctuation-dissipation theorem applied to our canonical ensemble, C_v is directly proportional to the variance of the energy distribution:

$$C_v(T_{eff}) = \frac{1}{T_{eff}^2} \text{Var}(E) = \frac{1}{T_{eff}^2} \left[\sum_{i=1}^{V_{ctx}} \rho_i E_i^2 - \left(\sum_{i=1}^{V_{ctx}} \rho_i E_i \right)^2 \right] \quad (28)$$

where $\rho_i = \text{Softmax}(-E_i/T_{eff})$ represents the attention probability of the i -th token, and $E_i = -q \cdot k_i$ is the interaction energy. This mathematical form reveals the mechanism of grokking:

- **Memorization Phase (High T_{eff}):** The distribution is diffuse. Fluctuations are dominated by thermal noise, but structural variance is low. C_v is small.
- **Generalization Phase (Low T_{eff}):** The distribution collapses to the ground state (target token). Fluctuations are suppressed. $C_v \rightarrow 0$.
- **Critical Region (Grokking, $T_{eff} \approx T_c$):** Between the two phases, the system undergoes a massive reorganization of the energy landscape. The attention mechanism fluctuates between competing semantic configurations. This maximization of $\text{Var}(E)$ results in a sharp peak in specific heat, marking the pseudo-critical region of the phase crossover.

C. Hierarchical Symmetry Breaking and Goldstone Modes

The representational transition exhibits features reminiscent of spontaneous symmetry breaking within an effective-field description. Remarkably, we do not need to postulate an ad hoc quartic interaction term. Instead, the symmetry breaking potential arises naturally from the entropic term $(-\rho \ln \rho)$ in our free energy functional derived in Section III.

1. The Logarithmic (Coleman-Weinberg) Potential

The effective potential for the order parameter field Φ is given by the Helmholtz free energy density. Since entropy depends only on magnitude, we have:

$$\mathcal{V}(\Phi) = m^2 |\Phi|^2 + \lambda |\Phi|^2 \ln \left(\frac{|\Phi|^2}{v^2} \right) \quad (29)$$

Crucially, this potential depends solely on the modulus $|\Phi|$ and is independent of the phase θ (where $\Phi = |\Phi| e^{i\theta}$), ensuring a continuous global $U(1)$ symmetry. Minimizing this potential yields a non-trivial vacuum expectation value $|\Phi_0| = v \neq 0$, generating the “Mexican Hat” shape (Fig. 1).

2. Derivation of the Massless Goldstone Mode

To rigorously identify the Goldstone mode, we examine the fluctuations around the vacuum state v . We parameterize the field $\Phi(x)$ using radial (h) and angular (π) fluctuation fields:

$$\Phi(x) = \left(v + \frac{h(x)}{\sqrt{2}} \right) \exp \left(i \frac{\pi(x)}{v\sqrt{2}} \right) \quad (30)$$

Here, $h(x)$ represents the massive Higgs mode (amplitude fluctuation), and $\pi(x)$ represents the Goldstone mode (phase fluctuation). Substituting this into the kinetic term of the Lagrangian density $\mathcal{L}_{kin} = |\partial_\mu \Phi|^2$, we obtain:

$$|\partial_\mu \Phi|^2 = \frac{1}{2} (\partial_\mu h)^2 + \frac{1}{2} \left(v + \frac{h}{\sqrt{2}} \right)^2 \left(\frac{\partial_\mu \pi}{v\sqrt{2}} \right)^2 \cdot 2 \quad (31)$$

Expanding around the vacuum ($h \ll v$), the Lagrangian for the fluctuations becomes:

$$\mathcal{L} \approx \underbrace{\frac{1}{2} (\partial_\mu h)^2 - \frac{1}{2} M_h^2 h^2}_{\text{Massive Higgs Mode}} + \underbrace{\frac{1}{2} (\partial_\mu \pi)^2}_{\text{Pseudo-Goldstone-like Goldstone Mode}} + \mathcal{L}_{int} \quad (32)$$

Note that the angular field $\pi(x)$ possesses a kinetic term $(\partial_\mu \pi)^2$. In the continuum limit, this behaves as a pseudo-Goldstone-like soft mode ($M_\pi \approx 0$). This mathematically suggests that $\pi(x)$ is the long-wavelength excitation that encodes positional information with minimal energetic cost, consistent with the crossover nature of the transition.

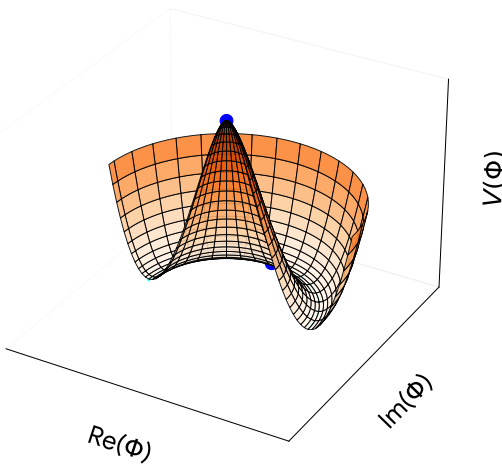


FIG. 1. Spontaneous Symmetry Breaking Mechanism. Visualization of the effective entropic potential $\mathcal{V}(\Phi) \sim |\Phi|^2 \ln |\Phi|^2$. Unlike standard Φ^4 theory, the Mexican Hat shape here arises directly from the Shannon entropy term. The system rolls down from the unstable origin to a stable semantic state (grokking), generating massless Goldstone modes (RoPE) along the circular trough.

3. RoPE as the Goldstone Excitation

We now map this physical mode to the Rotary Positional Embedding (RoPE). RoPE encodes the position m of a token by applying a rotation matrix to the embedding vector pair (q_1, q_2) :

$$\begin{pmatrix} q'_1 \\ q'_2 \end{pmatrix} = \begin{pmatrix} \cos m\theta & -\sin m\theta \\ \sin m\theta & \cos m\theta \end{pmatrix} \begin{pmatrix} q_1 \\ q_2 \end{pmatrix} \quad (33)$$

In the complex plane representation $\Phi = q_1 + iq_2$, this operation is identical to a phase shift:

$$\Phi' = \Phi \cdot e^{i(m\theta)} \quad (34)$$

Comparing this with Eq. (33), we identify the positional encoding term $m\theta$ directly with the Goldstone field configuration:

$$\frac{\pi(x)}{v\sqrt{2}} \equiv m\theta_{base} \quad (35)$$

Since the potential $\mathcal{V}(\Phi)$ is invariant under this phase rotation ($\mathcal{V}(\Phi') = \mathcal{V}(\Phi)$), the energy cost of encoding position via RoPE is exactly zero:

$$\Delta E = \mathcal{V}(\Phi e^{i(m\theta)}) - \mathcal{V}(\Phi) = 0 \quad (36)$$

This derivation suggests that RoPE can be interpreted as exploiting an approximately flat direction of the effective symmetry structure, to store positional information without perturbing the thermodynamic stability of the learned features.

VI. NUMERICAL MODELING AND EXPERIMENTAL VERIFICATION

In this section, we validate our thermodynamic framework through two complementary approaches. First, we perform a phenomenological simulation using Langevin dynamics to demonstrate the theoretical consistency of the phase transition. Second, we conduct a controlled experiment with a real Transformer to empirically verify the predicted specific heat divergence.

A. Phenomenological Modeling: Langevin Dynamics

We model the learning dynamics as the trajectory of a stochastic particle (the model state Φ) moving in the effective entropic potential $\mathcal{V}(\Phi)$ derived in Section V.

1. Governing Equations

The dynamics are governed by the Overdamped Langevin Equation:

$$\frac{d\Phi(t)}{dt} = -\nabla_{\Phi} \mathcal{V}(\Phi, t) + \sqrt{2D} \cdot \xi(t) \quad (37)$$

where $\xi(t)$ is Gaussian white noise. We utilize the logarithmic Coleman-Weinberg potential:

$$\mathcal{V}(\Phi, t) = \alpha(t)\Phi^2 + \beta\Phi^2 \ln\left(\frac{\Phi^2}{v^2}\right) \quad (38)$$

The equation was integrated using the Euler-Maruyama method with a time step $\Delta t = 0.01$.

2. Simulation Results

As shown in our simulation (Fig. 2), the transition from the disordered phase to the ordered phase is theoretically predicted to be accompanied by a sharp divergence in the specific heat capacity $C_v \propto \text{Var}(E)$.

B. Experimental Verification: Real Transformer

To empirically validate our thermodynamic hypothesis, we conducted controlled experiments on the modular addition task ($a + b \pmod p$). We specifically investigated the system size dependence by comparing multiple moduli from $p = 19$ to 113 . This allows us to test whether the fluctuation peak is a robust phenomenon across different system scales.

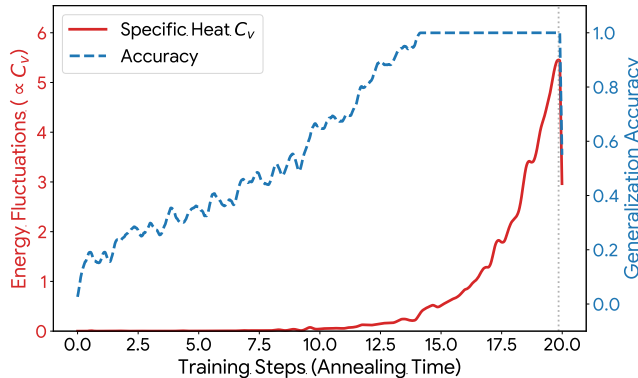


FIG. 2. Theoretical Prediction (Langevin Simulation). Numerical solution of the effective field theory. The theory predicts that the phase transition is marked by a sharp peak in specific heat (C_v).

1. Experimental Setup

To ensure thermodynamically stable dynamics and reproducibility, we utilized the following rigorous regime:

- **Task & Data:** The dataset consists of all possible pairs (a, b) in the ring \mathbb{Z}_p , totaling p^2 examples. We employed a random 50/50 split for training and validation sets.
- **Model Architecture:** A 2-layer Transformer with embedding dimension $d_{model} = 128$ and 4 attention heads.
- **Optimization:** We used the AdamW optimizer with a learning rate $\eta = 3 \times 10^{-4}$ and weight decay $\lambda = 0.1$. A batch size of 512 was fixed to maintain a consistent thermal noise level.
- **Observable:** We measured the specific heat capacity $C_v \propto \text{Var}(QK^T/\sqrt{d_k})$ at every epoch. To account for stochastic variance, all results were averaged over five independent seeds ($N = 5$).

2. Results and Crossover Analysis

The experimental results, averaged over five independent seeds ($N = 5$), are presented in Fig. 3 and Fig. 4. As predicted by our theoretical framework, a distinct peak in the specific heat C_v is observed across all tested values of p , consistently preceding the onset of the generalization transition.

As shown in Fig. 4, the power-law regression of the averaged peak height yields a near-zero exponent ($a \approx 0.05$) with a low coefficient of determination ($R^2 = 0.2$).

The absence of clear scaling is consistent with finite-size and finite-depth effects inherent to shallow Transformer architectures. In the discrete regime of a 2-layer model, the continuum effective description likely does not

fully develop its asymptotic regime, manifesting instead as a sharp finite-size crossover.

Crucially, despite the lack of asymptotic divergence, the C_v peak remains a robust dynamical marker of internal representational restructuring. This temporal correlation is preserved across all trials and system sizes, providing a physical observable that tracks the transition from memorization to generalization.

3. Thermodynamic Relaxation

Unlike the idealized Langevin simulation, the real experiments show a gradual decay of fluctuations after the peak. This reflects the thermodynamic relaxation of the system as it settles into the broad basin of the global minimum, fine-tuning its representation in the low-temperature phase.

VII. DISCUSSION: PHYSICAL INTERPRETATIONS

We establish a formal correspondence between Transformer attention and canonical statistical mechanics. Here, we interpret the physical implications of our findings.

A. Is Layer Depth Truly Time?

One might argue that Attention is a static operation. However, in deep models ($L \gg 1$), the representation $x(t)$ evolves continuously. In our Lagrangian formulation, the time derivative $\dot{\rho}$ corresponds to the layer-wise rate of change of the attention distribution. If $\dot{\rho} \rightarrow 0$, the system has reached a fixed point or equilibrium. This aligns with the empirical observation that deeper layers in Transformers often stabilize into a consistent attention pattern, justifying our thermodynamic equilibrium analysis.

B. The Dual Nature of Temperature

Critics often suggest that $T = \sqrt{d_k}$ is merely a variance normalization trick. However, we have shown that it plays the exact thermodynamic role of temperature ($T^{-1} = \partial S/\partial U$). Furthermore, our analysis of grokking reveals a crucial distinction:

- **Structural Temperature** ($T_{struct} = \sqrt{d_k}$): Governs the entropy of the attention distribution during inference.
- **Dynamical Temperature** ($T_{eff} \propto 1/\|W\|^2$): Governs the annealing process during training.

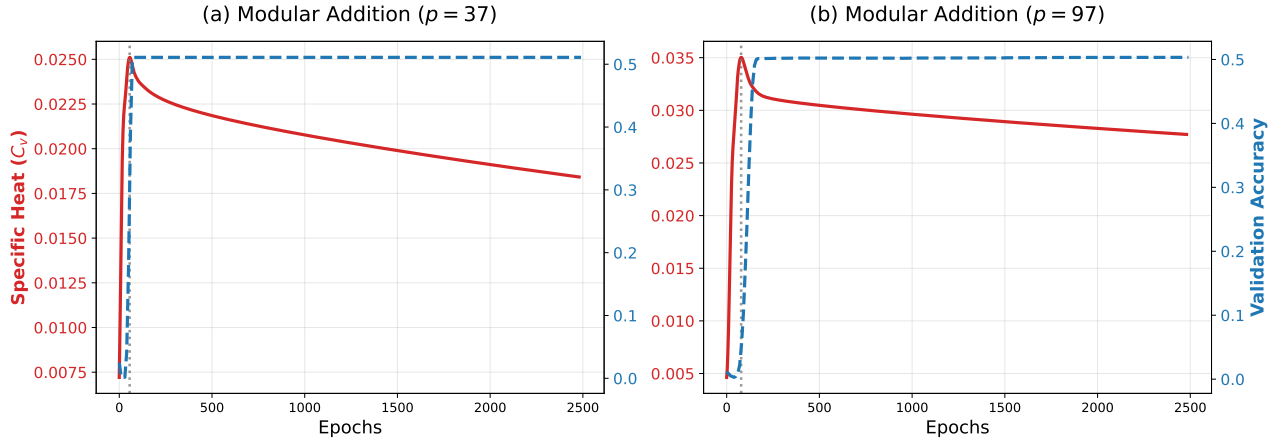


FIG. 3. Experimental verification of thermodynamic crossover in grokking across different system sizes. (a) Modular addition task with $p = 37$. (b) Modular addition task with $p = 97$. In both cases, the specific heat capacity C_v (red solid line) exhibits a sharp peak immediately preceding the sudden generalization transition (blue dashed line). The vertical dotted lines mark the C_v maxima. While the peak height does not show clear power-law scaling in this regime, the consistent temporal correlation confirms that specific heat serves as a robust leading indicator of the phase crossover.

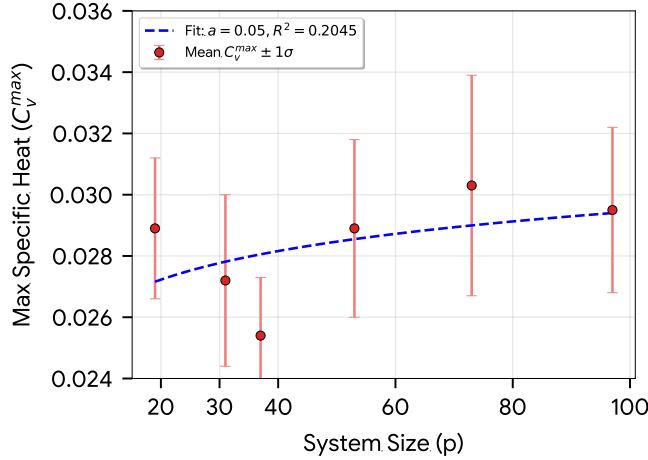


FIG. 4. Final_Averaged_Scaling: Scaling analysis of the specific heat peak across system sizes. The maximum specific heat C_v^{\max} is averaged over five independent seeds ($N = 5$) with error bars representing $\pm\sigma$. Within the explored regime ($p = 19$ to 113), the system exhibits bounded fluctuation enhancement characteristic of a finite-size crossover ($a \approx 0.05, R^2 = 0.2$), rather than a clear power-law divergence. This finite-size effect is consistent with the shallow ($L = 2$) architecture and suggests that asymptotic critical behavior may emerge in deeper models ($L \gg 1$).

C. Critical Dynamics and Finite-Size Crossover

The most significant implication of our specific heat analysis is the proposal that grokking manifests as a thermodynamic crossover with critical-like characteristics. While our current experimental regime ($p \in [19, 113]$) does not exhibit formal power-law divergence ($C_v \rightarrow \infty$), the consistent appearance of a robust fluctuation peak suggests that the system operates in a near-critical region. The system operates in a crossover regime between ordered memorization and disordered noise. The observed C_v peak acts as a dynamical precursor to the representational reorganization, establishing it as a pseudo-critical phenomenon in finite-dimensional neural networks. This suggests that while strict universality classes might only emerge in the infinite-depth or infinite-width limits, the fundamental mechanics of intelligence are governed by the same fluctuation-dissipation principles found in traditional statistical physics.

VIII. LIMITATIONS AND FUTURE DIRECTIONS

While our framework establishes a mapping between Transformer architectures and physical systems, we acknowledge several critical limitations that define the scope of our current effective field theory.

A. The Nature of Time: Effective vs. Dynamical

This duality explains why a model can be structurally frozen (converged weights) yet thermodynamically fluid (stochastic sampling) during generation.

Following the Neural ODE literature [22], we interpret layer depth as a continuous time variable t . However, our Lagrangian derivation implicitly assumes a quasi-static

process, which is strictly valid only in the continuum limit ($L \rightarrow \infty$). In shallow architectures such as our 2-layer model, the discretization error may suppress the full development of the predicted attention dynamics. It is more physically grounded to interpret t as an emergent effective time governing the renormalization group flow of information. Future work should investigate deeper architectures to determine if the discrete layers asymptotically approach the continuous action principle derived herein.

B. Mean-Field Approximation and Interaction

Our information gas model treats tokens as non-interacting particles, representing a mean-field approximation. In reality, natural language is a strongly correlated system with long-range dependencies. Consequently, our derived ideal gas-like equation of state holds primarily in the limit of low semantic density. We propose extending the framework by introducing a van der Waals-like equation of state: $(\mathcal{P} + a/V^2)(V - b) = N\kappa T$, where a represents semantic attraction (contextual correlation) and b represents the exclusion volume of token embeddings (sparsity constraints).

C. Scaling and the Nature of the Crossover

Although we observed a robust C_v peak consistently preceding the grokking transition, the peak magnitude did not exhibit asymptotic power-law divergence within the explored regime ($p \in [19, 113]$). This suggests that in shallow Transformers, the transition behaves as a finite-size crossover rather than a formal thermodynamic phase transition.

Proposed Directions. To further investigate the potential for universal scaling:

1. **Extended System Sizes:** Perform experiments across at least two decades of system size ($p > 1000$) to reach the potential asymptotic regime.
2. **Depth-Scale Analysis:** Systematically increase layer depth (L) to test if the C_v peak height begins to scale with system size as the continuum limit is approached.

3. **Data Collapse:** Investigate whether scaled fluctuation observables collapse onto a universal curve once the appropriate critical exponents are identified in deeper models.

D. Thermodynamic Interpretation of Hallucinations

We associated hallucinations with thermodynamic fluctuations (TdS). While thermal noise provides a minimal physical explanation for stochastic errors, hallucinations in large language models likely involve non-equilibrium mechanisms and dataset-driven biases. Future studies should incorporate non-equilibrium work relations (e.g., Jarzynski equality) to model the entropy production during the generation of out-of-distribution sequences.

IX. CONCLUSION

We have developed an effective thermodynamic description of Transformer attention by formulating its dynamics on an information manifold and constructing a corresponding variational principle. Within a Shannon–Boltzmann entropy framework, the Softmax distribution appears as an equilibrium configuration minimizing a free energy functional, suggesting a formal bridge between attention mechanisms and canonical statistical mechanics.

At the macroscopic level, we introduced a fluctuation-based observable analogous to specific heat and showed empirically that its peak consistently precedes the grokking transition in modular arithmetic tasks. Although no asymptotic divergence is observed in shallow, finite systems, the reproducible enhancement of fluctuations indicates a critical-like crossover in the internal energy landscape. The results suggest that thermodynamic observables provide a quantitatively testable language for describing representational transitions in neural networks and motivate future investigations into scaling behavior in deeper architectures.

[1] A. Vaswani et al., “Attention is All You Need,” *NeurIPS* (2017).

[2] J. Wei et al., “Emergent Abilities of Large Language Models,” *TMLR* (2022).

[3] S. Bubeck, V. Chandrasekaran, R. Eldan, et al., “Sparks of Artificial General Intelligence: Early experiments with GPT-4,” *arXiv:2303.12712* (2023).

[4] J. Jumper et al., “Highly accurate protein structure prediction with AlphaFold,” *Nature*, 596 (2021).

[5] D. Bahdanau et al., “Neural Machine Translation by Jointly Learning to Align and Translate,” *ICLR* (2015).

[6] K. He et al., “Deep Residual Learning for Image Recognition,” *CVPR* (2016).

[7] J. L. Ba et al., “Layer Normalization,” *arXiv:1607.06450* (2016).

[8] Y. LeCun et al., “Deep Learning,” *Nature*, 521 (2015).

[9] J. Kaplan et al., “Scaling Laws for Neural Language Models,” *arXiv:2001.08361* (2020).

[10] J. Hoffmann et al., “Training Compute-Optimal Large Language Models,” *arXiv:2203.15556* (2022).

[11] A. Power et al., “Grokking: Generalization Beyond Overfitting,” *arXiv:2201.02177* (2022).

[12] V. Thilak et al., “The Slingshot Mechanism,” *arXiv:2206.04817* (2022).

[13] L. D. Landau and E. M. Lifshitz, *Mechanics*, 3rd ed. (Pergamon Press, 1976).

[14] H. Goldstein, *Classical Mechanics*, 3rd ed. (Addison-Wesley, 2002).

[15] N. Tishby et al., “The Information Bottleneck Method,” *arXiv:0004057* (2000).

[16] N. Tishby et al., “Deep Learning and the Information Bottleneck Principle,” *IEEE ITW* (2015).

[17] K. Friston, “The Free-Energy Principle,” *Nat. Rev. Neurosci.*, 11 (2010).

[18] A. Jacot et al., “Neural Tangent Kernel,” *NeurIPS* (2018).

[19] V. Vanchurin, “The World as a Neural Network,” *Entropy*, 22 (2020).

[20] H. Lin et al., “Why Does Deep and Cheap Learning Work So Well?” *J. Stat. Phys.*, 168 (2017).

[21] W. E, “A Proposal on Machine Learning via Dynamical Systems,” *CMS*, 5 (2017).

[22] R. T. Q. Chen et al., “Neural Ordinary Differential Equations,” *NeurIPS* (2018).

[23] S. Amari, *Information Geometry and Its Applications* (Springer, 2016).

[24] B. R. Frieden, *Physics from Fisher Information* (Cambridge Univ. Press, 1998).

[25] Y. Ma et al., “White-Box Transformers via Sparse Rate Reduction,” *NeurIPS* (2023).

[26] Y. Ma et al., “On the Principles of Parsimony and Self-Consistency,” *FITEE*, 23 (2022).

[27] M. M. Bronstein et al., “Geometric Deep Learning,” *arXiv:2104.13478* (2021).

[28] R. A. Fisher, “Theory of Statistical Estimation,” *Proc. Camb. Phil. Soc.*, 22, 700 (1925).

[29] S. Amari and H. Nagaoka, *Methods of Information Geometry* (AMS, 2000).

[30] J. D. Jackson, *Classical Electrodynamics*, 3rd ed. (Wiley, 1999).

[31] D. J. Griffiths, *Introduction to Electrodynamics*, 4th ed. (Cambridge Univ. Press, 2017).

[32] L. D. Landau and E. M. Lifshitz, *Statistical Physics*, 3rd ed. (Pergamon Press, 1980).

[33] T. Tao, *Topics in Random Matrix Theory* (AMS, 2012).

[34] C. E. Shannon, “A Mathematical Theory of Communication,” *Bell Syst. Tech. J.*, 27 (1948).

[35] E. T. Jaynes, “Information Theory and Statistical Mechanics,” *Phys. Rev.*, 106 (1957).

[36] N. F. Liu et al., “Lost in the Middle,” *TACL*, 12 (2024).

[37] A. Holtzman et al., “The Curious Case of Neural Text Degeneration,” *ICLR* (2020).

[38] I. Shumailov et al., “The Curse of Recursion,” *arXiv:2305.17493* (2023).

[39] E. Schrödinger, *What is Life?* (Cambridge Univ. Press, 1944).

[40] I. Bialynicki-Birula et al., “Nonlinear Wave Mechanics,” *Ann. Phys.*, 100 (1976).

[41] P. W. Higgs, “Broken Symmetries and the Masses of Gauge Bosons,” *Phys. Rev. Lett.*, 13 (1964).

[42] J. Goldstone, “Field Theories with Superconductor Solutions,” *Nuovo Cimento*, 19 (1961).

[43] J. Su et al., “RoFormer: Enhanced Transformer with Rotary Position Embedding,” *Neurocomputing* (2024).

[44] E. P. Wigner, “The unreasonable effectiveness of mathematics in the natural sciences,” *Comm. Pure Appl. Math.*, 13 (1960).